Available online at www.sciencedirect.com

ScienceDirect

Procedia Manufacturing 00 (2017) 000–000

Procedia MANUFACTURING

www.elsevier.com/locate/procedia

27th International Conference on Flexible Automation and Intelligent Manufacturing, FAIM2017, 27-30 June 2017, Modena, Italy

# Virtual Prototyping of a Flexure-based RCC Device for Automated Assembly

V. Vaschieri[2], M. Gadaleta[2], P. Bilancia[1], G. Berselli[1]*, R. Razzoli[1]

[1]*Department of Mechanics, Energetics, Management and Transportation,University of Genova, Via All'Opera Pia, 15/A, 16145 Genova, Italy*
[2] *"Enzo Ferrari" Department of Engineering, University of Modena and Reggio Emilia, Via P. Vivarelli, 10, 41125 Modena, Italy*

**Abstract**

The actual use of Industrial Robots (IR) for assembly systems requires the exertion of suitable strategies allowing to overcome shortcomings about IR poor precision and repeatability. In this paper, the practical issues that emerge during common "peg-in-hole" assembly procedures are discussed. In particular, the use of passive Remote Center of Compliance (RCC) devices, capable of compensating the IR non-optimal performance in terms of repeatability, is investigated. The focus of the paper is the design and simulation of a flexure-based RCC that allows the prevention of jamming, due to possible positioning inaccuracies during peg insertion. The proposed RCC architecture comprises a set of flexural hinges, whose behavior is simulated via a CAE tool that provides built-in functions for modelling the motion of compliant members. For given friction coefficients of the contact surfaces, these numerical simulations allow to determine the maximum lateral and angular misalignments effectively manageable by the RCC device.

Peer-review under responsibility of the scientific committee of the 27th International Conference on Flexible Automation and Intelligent Manufacturing.

*Keywords:* Virtual Prototyping; Robotic assembly; Peg-in-hole assembly; Compensation Strategies; RCC Device; Compliant Flexures

## 1. Introduction

Facing assembly processes using anthropomorphic Industrial Robots (IR) implies the build-up of a "*high-tech work area*", where a strong cooperation between the robot itself and all the auxiliary equipment/component is enabled. As compared to operations performed by human workers, the main difficulties of an Automated Assembly Process (AAP)

* Corresponding author. Tel.: (+39) 010 353-2839; *E-mail address:* giovanni.berselli@unige.it


Peer-review under responsibility of the scientific committee of the 27th International Conference on Flexible Automation and Intelligent Manufacturing.

are related to the imperfections in the relative positioning of the parts to be mated. In fact, despite any source of imperfection, manual operators can easily handle the task thanks to their ability of precisely compensating positioning errors, the capability of sense and react to excessive contact forces (i.e. load control), and the inherent variable compliance of the human hand (i.e. stiffness control during contacts) [1,2]. Ideally, if an assembly cell operating in a structured environment could guarantee high-precision parallel alignment between the mating surfaces, the parts to be mated being always identical and perfectly manufactured, the assembly task could be successfully completed without the aid of error-compensation strategies. On the other hand, the IR limited precision/accuracy, the dimensional/geometric tolerances of the parts, the dimensional and mounting errors in the jig and fixture systems [3], along with the existence of time-dependent phenomena, such as components wear and dependency on external (uncontrollable) factors, require to be carefully considered whenever designing and commissioning a robotized assembly cell. Similarly to other IR-based manufacturing processes (such as robotic deburring [4]), the error sources in an AAP may be classified as follows:

- *Robot-dependent sources*, which may be furtherly classified into geometrical and non-geometrical errors [5,6]. Geometrical errors are due to imperfect geometries and mating/assembly inaccuracies within the IR structure, leading to a discrepancy between predicted and actual (static) TCP pose. Non-geometrical errors arise only during the IR motion. They include un-modeled dynamic effects which are not compensated by the traditional IR controller, such as non-linear joint stiffness, backlash in the gear reducers, stick-slip friction effects, and structural deformations. In practice, from a nomenclature standpoint, precision is frequently used as a crucial IR performance measure; it consists of repeatability, accuracy and resolution. For what concerns assembly tasks, repeatability may be regarded as more important than accuracy, since it is possible to improve the latter by properly programming the IR path. Typical values of IR accuracy are in the range of ± 1 mm, although values of 0.3 mm can be reached with an accurate compensation [7].
- *External and environmental sources*, such as temperature-dependent disturbances [8], deflections/vibrations of the robot base attachment, and non-ideal behaviour of any auxiliary device located within the cell. For instance, a temperature increase due to friction in the sliding parts and actuators' functioning leads to non-negligible and hardly quantifiable deformations, since the IR components are characterized by different thermal expansion coefficients and complex geometries.
- *System and process-dependent errors*, the first being due to an improper IR calibration, errors within the sensors measurements and/or numerical approximations performed by the computer that manages the control, the latter coming from time-varying external forces acting on the IR end-effector. For instance, in the case of AAP or robotic deburring/machining, the forces exchanged at the robot TCP (henceforth causing undesired deflection, namely robot-dependent errors) are mainly generated as a result of contacts [9].

Owing to these considerations, it is rather obvious that the abovementioned sources of uncertainty in AAP need to be addressed via purposely chosen compensation strategies. Since perfect part positioning cannot be practically achieved and, in any case, the variability due to the tolerances in the mating parts is unavoidable, two main error compensation methods have been widely studied in the literature [2], namely *passive compensation*, based on non-rigid devices connected to the robot flange, or *active compensation*, based on the use of force/torque sensors mounted on the IR flange (Fig. 1). As for the latter method, several experimental studies have been reported in numerous publications (see e.g. [10] for more references). As for the first method, most of the previous work deals with the well-known *Remote Center of Compliance* (RCC) mechanism, namely a commercially available device whose advantages and drawbacks for AAP as compared to solution for active compensation have been clearly discussed in [11]. In the past, a number of RCC design solutions has been described. For instance, an RCC employing four elastic beams, along with a procedure for determining the optimal beam parameters is reported in [12]. A solution comprising two compliant four-bar-linkage mechanisms has been described in [13], whereas hybrid solutions (i.e. sensorized RCC) have been proposed in [14], in the attempt to combine the advantages of passive and active compensation strategies. For what concerns RCC analytical modelling, accurate models employing the method of the screw theory are reported in [15], whereas an analytical analysis of the forces arising during assembly of parts with simplified geometry (e.g. chamferless cylindrical parts) are reported in [10]. These kind of analysis have also been performed for parts lacking rotational symmetry about their major axis [16].

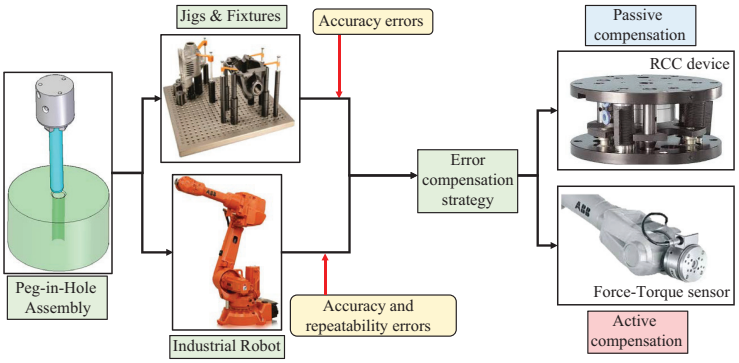


Fig. 1. Peg-in-hole assembly: a schematic of error sources and compensation strategies.

Within the scenario, the purpose of the present work is to describe the design and simulation of a flexure-based RCC to be used in common *peg-in-hole* assembly task. The proposed RCC comprises a couple of flexure-based four-bar-linkage mechanisms, characterized by a compliant structure whose elastic deformation is localized in "small regions", the term *flexure* being used to indicate the location at which the deflection is concentrated. The proposed mechanism is analyzed via non-linear Finite Element Method (FEM) and then by means of the Pseudo-Rigid-Body-Model (PRBM) approach [17,18]. Generically speaking, a PRBM describes a compliant mechanism by a series of rigid links connected through spring-loaded kinematic joints, its advantages over FEM analysis being a significant reduction of the computational costs for the numerical analysis. As clearly highlighted in [19], PRBM have been successfully employed for evaluating the workspaces of several inherently compliant devices [20], for designing non-linear springs [21], and for analyzing the dynamic behavior of systems comprising compliant elements [22,23]. For what concerns the engineering tools employed during design and simulation activities, the software *Solidworks* has been used for the computer-aided-design of the parts, whereas the software *Recurdyn* has been used to simulate the overall peg-in-hole assembly process. Differently from an analytical approach, this method leverages on the capabilities of general-purpose CAE tools and allows to quickly simulate the peg-in-hole insertion at varying friction coefficients between parts and insertion speed. For a specific case study (i.e. insertion of cylindrical chamfered peg into a chamfered hole) and given friction coefficients of the contact surfaces, these numerical simulations allow to determine the maximum allowable lateral and angular misalignments, effectively manageable by the RCC device. The results are summarized in a set of tables that depict the feasibility of the assembly process, once the part tolerances are defined.
The rest of the paper is organized as follows: Section 2 briefly recalls basic background about the structure of RCC devices; Section 3 describes the main features of the proposed flexure-based RCC; Section 4 describes the creation of the overall RCC virtual prototype and provides simulation results; Section 5 reports the concluding remarks.

## 2. Basic Background on Peg-in-Hole assembly via RCC devices

The use of a passive compensation device for AAP is closely related to the type of parts to be mated. In the following, as a particular case, the most common "peg-in-hole" assembly procedure is considered [1]. As depicted in Fig. 2, let us focus on a cylindrical pin with length $l$ and diameter $d$, having chamfered ends characterized by width $w$ and height $c$, the corresponding inclination angle being indicated as $\alpha$. The pin shall be inserted into a chamfered hole of diameter $D$, the chamfer dimensions being $W$x 45°. The minimum clearance between the pin and hole (as specified by the parts tolerances) is indicated as $g$.

Owing to the prescribed mating clearance, parts assembly can be easily carried out in the ideal condition in which pin and hole vertical axis are perfectly aligned (as depicted in Fig. 2b). On the other hand, during practical AAP, possible misalignments may rise, which may be defined as follows:

- *Lateral Misalignment* (LM), as depicted in Fig. 2c, which corresponds to a situation in which pin and hole axes of symmetry are parallel but not collinear.
- *Angular Misalignment* (AM), as depicted in Fig. 2d, which corresponds to a situation in which pin and hole axes of symmetry intersect at a certain point.
- Combined *Lateral and Angular Misalignment*, as depicted in Fig. 2e, where both LM and AM are contemporarily involved in the AAP.

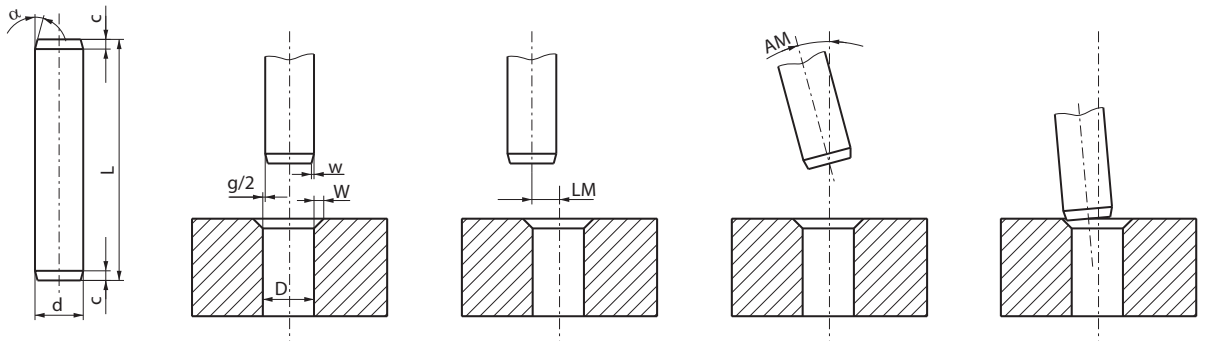


a) Pin dimensions. b) Pin and hole dimensions. c) Lateral misalignment (LM). d) Angular misalignment (AM). e) Combined lateral and angular misalignment.

Fig. 2. Pin and hole dimensions and definition of possible misalignments.

In the latter case, as described in and schematized in Fig. 3a, the possible phases of a generic pin insertion may be defined as *chamfer crossing*, *one-point contact*, *two-point contact* and *line contact*. Although not all the four phases may be present in all assembly procedure, this schematic represents a rather common situation, which have been described through several, two-dimensional theoretical models, whose aim is to predict the assembly feasibility [11-13,24]. In particular, the first contact occurs on the pin and hole chamfer. During the chamfer crossing phase, the contact location moves laterally in order to eliminate the lateral misalignment, the pin being pushed by the contact force. The contact location then reaches the pin rim (one-point contact) and, eventually, a second contact point occurs on the opposite side as the insertion proceeds. During the two-contact phase, the mating parts attempt to rotate with respect to each other in order to eliminate the angular misalignment. In some cases, the two point-contact phase may be followed by the line-contact phase, pin and hole being in contact along one wall. During the two-contact phase, two well-known failure modes may occur, namely *wedging* and *jamming* [25,26]. Wedging is an irremediable condition which describes a configuration such that every possibly force is in equilibrium with the contact forces, the only practical solution to the problem being a limitation of the AM value. Jamming occurs when the applied insertion force is balanced by friction reaction forces. Jamming can be avoided via either active compensation or by passive devices, such as the RCC, namely a mechanical spring structure (attached to the IR end-effector) that holds the pin to be assembled. In its simplest form, a RCC schematic is reported in Fig. 4. The devices comprise two parts, respectively responding to lateral loads and angular loads. The first part responds to lateral contact forces by moving laterally without rotating by means of a parallelogram four bar linkage. The second part responds to torques (still due to contacts) by performing small rotations about a remote centre of compliance located near the tip of the peg. As previously stated, some attempts have been made in order to provide RCC design with adaptable parameters (e.g. variable compliance or adjustable position of the remote center [2]).

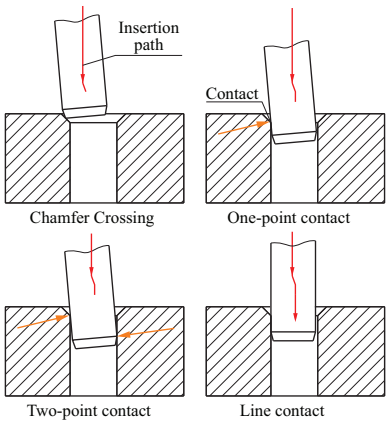


Fig. 3. Phases of the pin assembly process, location of the contact forces, and representation of the pin insertion path.

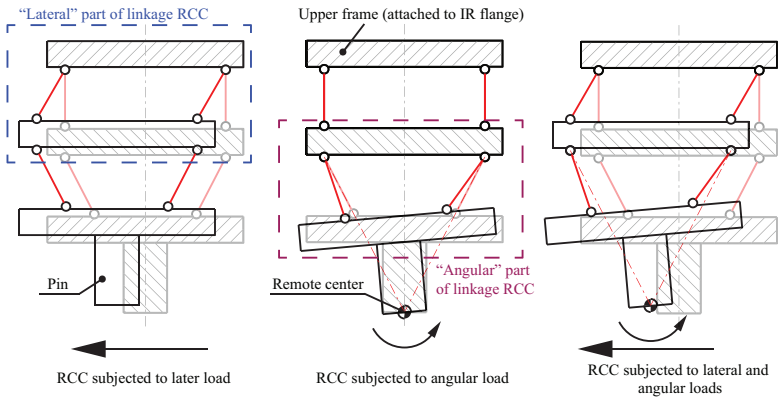


Fig. 4. Planar representation of a common RCC device: "Lateral" (translational) RCC part responding to later loads, "Angular" (rotational) RCC part responding to angular loads, and combined action of lateral/angular loads.

## 3. Design of the flexure-based RCC device

The idea on the basis of this paper is to simplify a classic RCC device by leveraging on the "compliant mechanism" concept [17]. Potential advantages over traditional mechanisms can be outlined into *cost reduction* and *increased performance*. In fact, compliant mechanisms require fewer components to achieve the desired mobility with consequent reduction of time/cost for the device manufacturing. For what concerns possible performance improvement, the absence of rigid kinematic pairs reduces wear, need of lubrication and possible backlash, which might be beneficiary in terms of mechanism precision. In the following, as a possible design choice, a flexure-based device has been developed. As widely known, flexure-based compliant mechanisms are structures characterized by the capability of providing elastic deformation localized in "small regions", the term *flexural joint* or *flexure* being used to indicate the location at which the deflection is concentrated.

The 3D CAD model of the device is shown in Fig. 5a, whereas Fig. 5b and 5c respectively depict the lateral and the angular part of the RCC. The main features of the device may be outlined as follows:

- Presence of three symmetrically disposed cylindrical rods (i.e. rods $A_r$, $B_r$, $C_r$ shown in Fig. 4b) connecting upper and lower frame (lateral RCC part) and thee symmetrically disposed rods (i.e. rods $D_r$, $E_r$, $F_r$ shown in Fig. 4c) connecting lower and intermediate frame (angular RCC part). The intermediate frame is connected to a gripper that holds the pins to be assembled, whereas the upper frame is connected to the IR flange.
- The cylindrical rods comprise variable cross sections. In practice, cylindrical corner-filleted flexures [18] are manufactured at both ends of the rods. From a kinematical standpoint, this flexure geometry is employed to mimic the behavior of a spherical joint (similarly to e.g. [27-30]).
- The frames are shaped so as to provide housing for the rods. With reference to Fig. 5c, for what concerns lower and intermediate frame, a set of three housing slots has been designed. This arrangement allows to easily change the inclination of the rods $D_r$, $E_r$ and $F_r$, thus allowing to either reduce or increase the distance of the remote center from the base of the lower frame. In practice, three working configurations are possible, each of which can be proven to be advantageous for assembling pins of a certain length, L (see Fig. 2a).

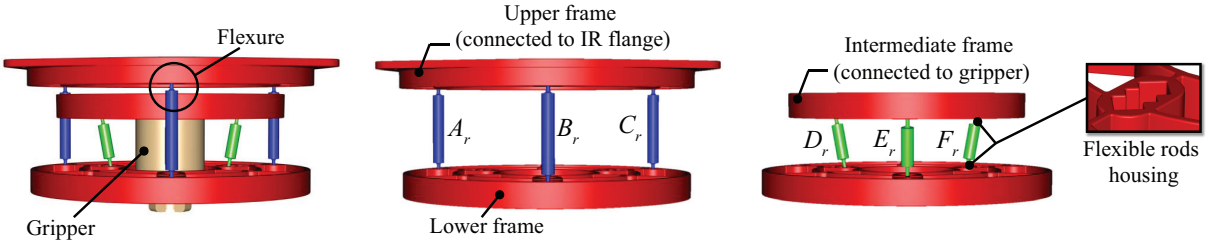


a) Overall flexure-based RCC device. b) "Lateral" part of the RCC device. c) "Angular" part of the RCC device.

Fig. 5. CAD model of the flexure-based RCC device: (a) overall device (including gripper); (b) "Lateral" RCC part; (c) "Angular" RCC part with side view of the rods' housings.

For what concerns the RCC manufacturing, all components are made of plastics. As suggested in [17,18], Delrin 100 NC010 has been chosen as suitable flexure material, since it provides a good $S_y/E$ ratio ($S_y$ being the material yield strength and $E$ being the material Young modulus). The flexure geometry is reported in Fig. 6, $l_f$, $d_f$, and $r_f$, being the flexure length, the diameter of the cylindrical cross section and radius of the base fillet. The same picture also shows the related PRBM, consisting of a spring-loaded spherical joint located in correspondence to flexure centroid (i.e. point $c_r$) and comprising three identical rotational springs mounted in parallel, These springs are characterized by rotational stiffness along the $x$, $y$, and $z$ (see Fig. 6, the $x$ axis being perpendicular to the $yz$ plane) denoted as $K_{\vartheta x} = K_{\vartheta y} = K_{\vartheta z}$. The overall virtual model of the proposed device, along with simulation results regarding peg-in-hole assemblies are reported in the next section.

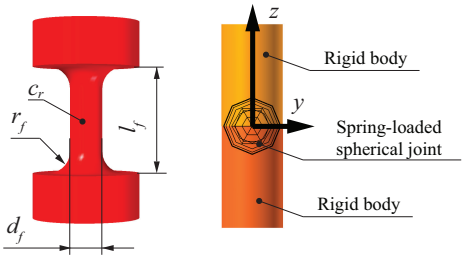


Fig. 6. Flexure dimensions and related PRBM.

## 4. Virtual Prototyping and Simulation Results

As a practical case, a peg-in-hole insertion process employing the proposed RCC device has been simulated within the *Recurdyn* environment. With reference to Figs. 2a and 2b, the pin dimensions are $d = 10\ mm$, $L = 80\ mm$, $c = 2\ mm$, $\alpha = 15°$, $w = 0.54\ mm$, whereas the hole dimensions are $D = 10.1\ mm$, $W = 1\ mm$. The clearance between peg and hole is easily computed as $g = D - d = 0.1\ mm$, whereas the maximum bearable $LM$ can be computed as $W + w + g/2 = 1.59\ mm$. At first, a model comprising meshed flexible elements has been simulated by employing the *Recurdyn* FEM solver and imposing lateral and angular misalignment values $LM = 1.5\ mm$ and $AM = 0.5°$. The overall model is depicted in Fig. 7, rods $D_r$, $E_r$, $F_r$ (Fig. 5c) being placed in such a way that the remote center is located on the pin tip. The flexure dimensions (see Fig. 6) are $d_f = 1.5\ mm$, $l_f = 5\ mm$ and $r = 1\ mm$. As for the rods material, the Young's modulus and Poisson's ratio are, respectively, $E = 2.9\ GPa$ and $\nu = 0.3$. Regarding the *Recurdyn* FEM model, a mapped mesh with brick elements has been defined (0.4 $mm$ as max element size). After a mesh convergence analysis, the employed mesh consists of 51971 tetra-4 elements and 11288 nodes for rods $A_r$, $B_r$, $C_r$, and 41754 tetra-4 elements and 9099 nodes for rods $D_r$, $E_r$, $F_r$. The Linear Elastic Model algorithm has been chosen in order to ensure a linear relationship between stresses and deformations. Concerning the contact parameters, the static and dynamic friction coefficients have been set to 0.78 and 0.42 respectively. A vertical motion with speed $0.5\ mm/s$ has been imposed to the upper frame, forcing the pin insertion.

After this first simulation, the PRBM of the proposed device has been set-up, the resulting *Recurdyn* model being shown in Fig. 8. The stiffness of the rotational springs has been computed by firstly analyzing a single flexure via FEM. In particular, the flexure has been treated as a cantilever beam loaded with a pure moment on its free-end and measuring the consequent free-end rotation (according to the procedure described in [21]). The resulting PRBM spring stiffness is $K_{\vartheta x} = K_{\vartheta y} = K_{\vartheta z} = 176\ Nmm/rad$. Friction coefficients, lateral and angular misalignments, and speed of the upper frame motion are maintained unvaried with respect to the previous simulation.

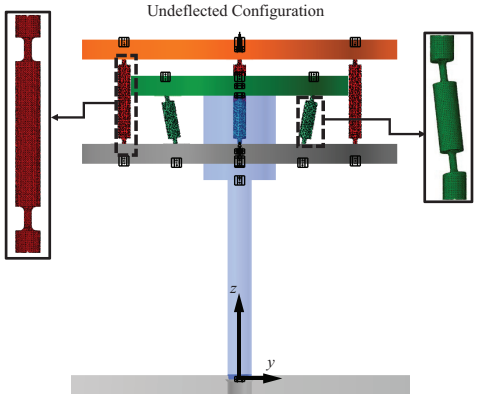


Fig. 7. RCC FEM model within the Recurdyn environment, showing the mesh of the flexible members.

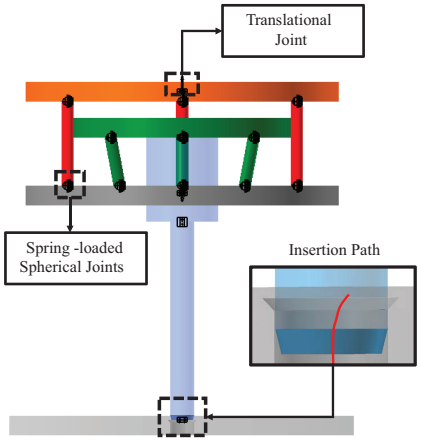


Fig. 8. RCC PRBM model within the Recurdyn environment, showing spring-loaded spherical joints and pin insertion path.

The numerical results concerning lateral and angular compensation values, measured in the $yz$ plane (Fig. 7), as function of time, are reported in Fig. 9. The same picture provides results coming from both FEM analysis and PRBM, confirming that the PRBM accurately captures these quantities of interest. Note that neither the lateral nor the angular compensations ever reach the values set for $LM$ and $AM$, since an imposed peg/hole clearance, $g$, is present and the models also capture possible 3D motions of the pin within the hole. As for the insertion force, Fig. 10 depicts the numerical results concerning the PRBM, also highlighting the various contact phases. With reference to Fig. 3, in the present case study, line contact is not reached, whereas the one-point and two-point contact phases, defined for a two-dimensional model, have been denoted as single-side and double-side contacts in order to highlight the 3D nature of the performed simulations. The shape of the curve closely replicates the theoretical results presented in [10]. Nonetheless, it is necessary to remark that the insertion force value strongly depends on the contact parameters set within the software, so that an accurate force prediction would surely require an experimental tuning.

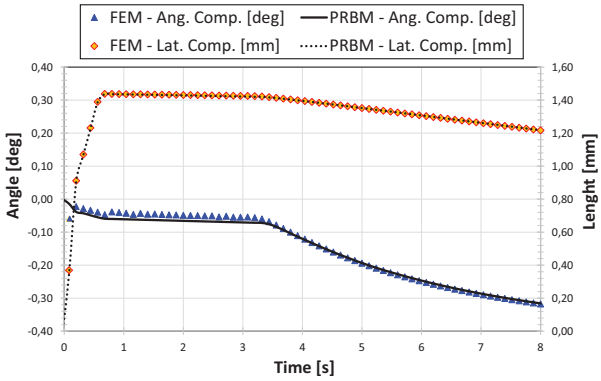


Fig. 9. Lateral and angular compensations provided by the RCC for $LM = 1.5\ mm$ and $AM = 0.5°$. FEM and PRB results.

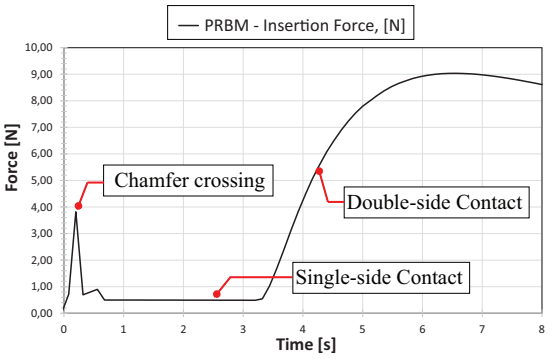


Fig. 10. Insertion force computed via PRBM, showing the various contact phases (see Fig. 3).

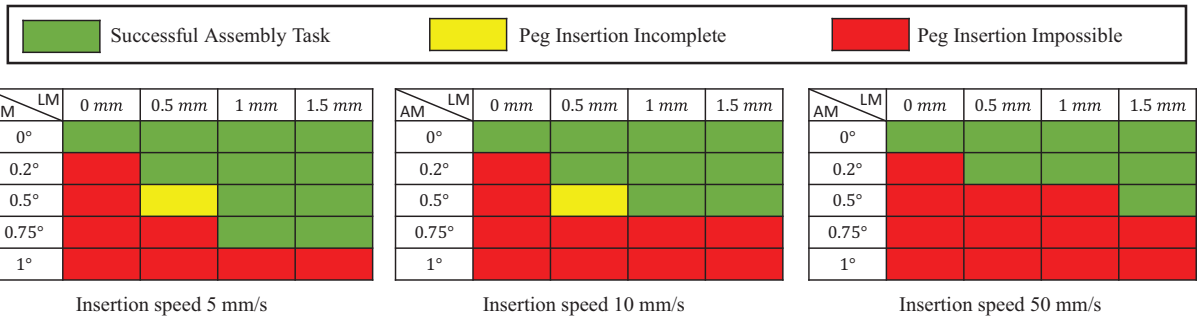


Fig. 11. RCC workspace for increasing insertion speed.

After the validation of the PRBM approach, another set of simulations have been performed for several $LM$ and $AM$ values and insertion velocities. In particular, LM values varying in the range $[0 \div 1.5]\ mm$, and AM values varying in the range $[0 \div 1]°$ have been considered, along with three insertion speeds equal to $5\ mm/s$, $10\ mm/s$ and $50\ mm/s$. The results are summarized in Fig. 11, which graphically shows whether or not the peg-in-hole assembly process has been feasible for a certain combination of misalignment errors and insertion speed. For what concerns computational times, all the models have been solved on a Notebook PC with an Intel I7-4719HQ CPU @ 2.50GHz and 16GB RAM. The FEM model is solved in about 600 min, whereas the PRBM is simulated in about 12 min.

## 5. Discussion and Conclusion

In this paper, a flexure-based RCC device has been presented. After the design of the mechanism, which allows to discretely vary the position of the remote center to three different values, a set of numerical simulations have been performed. At first, a quasi-static peg-in-hole assembly procedure has been simulated by employing FEM analysis (including the large deflections of the flexible members and the contact forces arising during peg insertion). Then, a PRBM has been considered, whose numerical results accurately replicate the system for what concerns the quantities of interest. The latter model allows to simulate the overall insertion process and to assess its feasibility. For given friction coefficients (taken from the literature), simulations have been performed at varying insertion speed and varying values of the angular/lateral misalignments between peg and hole symmetry axes. The advantages of the proposed method with respect to a theoretical analysis are: 1) capability to easily extend the feasibility study of the insertion process to problems requiring a three-dimensional model; 2) parametrization of the insertion speed; 3) low computational costs as compared to FEM analyses.

## 6. Acknowledgements

This research was funded by the Italian Ministry of research within the project 'Adaptive and modular approaches for the digital enabled factory', CTN01_00163_216730.

## References

[1] Bruzzone, L., Molfino, R., Zoppi, M. Modelling and control of peg-in-hole assembly performed by a translational robot. IASTED, International Conference Modelling, Identification and Control (MIC2002), Innsbruck, pp. 512-517, 2002.
[2] Brock, O., Kuffner, J., Xiao, J. Motion Manipulation for tasks. Springer Handbook of Robotics 1st ed. B. Siciliano and O. Khatib Eds. Berlin Heidelberg Germany, ch. 26 pp. 615-645, 2008.
[3] Hoffman, E.G. Jig and Fixture Design. Delmar Cengage Learning, 2012
[4] Morris, C. Robots for deburring. Advanced Manufacturing Technology, 33(11) pp. 6-8, 2012.
[5] Schneider, U. et al. Improving robotic machining accuracy through experimental error investigation and modular compensation. International Journal of Advanced Manufacturing Technology, 85(1), pp.3-15, 2016.
[6] Berselli, G. et al. Engineering Methods and Tools Enabling Reconfigurable and Adaptive Robotic Deburring. Advances on Mechanics, Design Engineering and Manufacturing, Lecture Notes in Mechanical Engineering, pp. 655-664, 2016.
[7] Mustafa, S.K., Pey, Y.T., Yang. G., Chen, I. A geometrical approach for online error compensation of industrial manipulator. IEEE/ASME AIM, International Conference on Advanced Intelligent Mechatronics, pp. 738-743, 2010.
[8] Simoni, L., Beschi, M., Legnani, G., Visioli, A. Friction modeling with temperature effects for industrial robot manipulators. IEEE/RSJ IROS, International Conference on Intelligent Robots and Systems, Hamburg, pp. 3524-3529, 2015.
[9] COMET Project – Plug-and-Produce COmponents and METhods for Adaptive Control of Industrial Robots Enabling Cost Effective, High Precision Manufacturing in Factories of the Future. European 7th Framework Programme, reference number 258769, http://www.cometproject.eu.
[10] Whitney, D.E. Mechanical Assemblies - Their Design, Manufacture, and Role in Product Development. Oxford Series on Advanced Manufacturing, 2004.
[11] Wang, W., Loh, R.N.K. Gu, E.Y. Passive compliance versus active compliance in robot-based automated assembly systems. Industrial Robot: An International Journal, 25(1), pp. 48-57, 1998.
[12] Lai, L.J., Zhu, Z.N. Modeling and Analysis of a Compliance Model and Rotational Precision for a Class of Remote Center Compliance Mechanisms. Applied Science, 6(388), 15 pages, 2016.
[13] Choi, B.J. et al. Design of orientation stages for step and flash imprint lithography. Precision Engineering, 25, pp. 192-199, 2001.
[14] Bright, G., Deubler, C. Design and Implementation of an Intelligent Remote Centre Compliance (IRCC) as a means of intelligent position feedback for a construction robot. Automation and Robotics in Construction, pp. 1-5, 1999.
[15] Ciblak, N., Lipkin, H. Design and Analysis of Remote Center of Compliance Structures. Journal of Robotic Systems, 20(8), pp. 415-427, 2003.
[16] Caine, M.E., Lozano-Perez, T. Seering, W. P. Assembly strategies for chamferless parts. IEEE ICRA, International Conference on Robotics and Automation, Scottsdale, vol. 1, pp. 472-477, 1989.
[17] Howell, Larry L. Compliant mechanisms. John Wiley & Sons, 2001
[18] Lobontiu, N. Compliant Mechanisms: Design of Flexure Hinges. CRC Press, 2002.
[19] Chen, G., Botao X., and Xinbo H. Finding the optimal characteristic parameters for 3R pseudo-rigid-body model using an improved particle swarm optimizer. Precision Engineering 35(3), pp. 505-511, 2011.
[20] Midha A, Howell L.L, Norton T.W. Limit positions of compliant mechanisms using the pseudo-rigid-body model concept. Mechanisms and Machine Theory, 35(1), pp. 99-115, 2000.
[21] Berselli, G., Meng, Q., Vertechy, R., Parenti Castelli, V. An improved design method for the dimensional synthesis of flexure-based compliant mechanisms: optimization procedure and experimental validation. Springer Meccanica, 51(5) pp. 1-17, 2016.
[22] Yu Y.Q., Howell L.L., Lusk C., Yue Y., He M.G. Dynamic modeling of compliant mechanisms based on the pseudo-rigid-body model. ASME Journal of Mechanical Design, 27(7), pp. 760-765, 2005.
[23] Berselli, G., Vertechy, R., Babič, M., Parenti Castelli, V. Dynamic modeling and experimental evaluation of a constant-force dielectric elastomer actuator. Journal of Intelligent Material Systems and Structures, 24(6), pp. 779-791, 2013.
[24] Whitney, D.E. Quasi-Static Assembly of Compliantly Supported Rigid Parts. *A*SME Journal of Dynamic Systems, Measurements and Control, 104(1), pp. 65-77, 1982.
[25] Dupont, P.E., Yamajako, S.P. Jamming and wedging in constrained rigid-body dynamics. IEEE ICRA, International Conference on Robotics and Automation, pp. 1-6, 1994.
[26] Simunovic, S.N. Force information in assembly processes. Proceedings of the 5th International Symposium in Industrial Robots, pp. 415-431, 1975.
[27] Tanık, E., Parlaktaş, V. A new type of compliant spatial four-bar (RSSR) mechanism. Mechanism and Machine Theory, 46(5), pp. 593-606, 2011.
[28] Tanik, E., Parlaktaş, V. Fully compliant spatial four-bar mechanism. Journal of Advanced Mechanical Design, Systems, and Manufacturing, 9(1), pp. 1-12, 2015.
[29] Berselli, G., Piccinini, M., Vassura, G. Comparative evaluation of the selective compliance in elastic joints for robotic structures. IEEE International Conference on Robotics and Automation, pp. 4626-4631, 2011.
[30] Berselli, G., Guerra, A., Vassura, G., Andrisano, A.O. An engineering method for comparing selectively compliant joints in robotic structures. IEEE/ASME Transactions on Mechatronics, 19(6), pp. 1882-1895, 2014.